Crystals of the *Chlamydomonas reinhardtii* Cell Wall: Polymerization, Depolymerization, and Purification of Glycoprotein Monomers

Ursula W. Goodenough,* Brian Gebhart,* Robert P. Mecham,‡ and John E. Heuser§

*Department of Biology, ‡Pulmonary Division, and §Department of Cell Biology/Physiology, Washington University, St. Louis, Missouri 63130

Abstract. Two of the three major outer layers of the *Chlamydomonas reinhardtii* cell wall (W6 and W4) can be solubilized from living cells with sodium perchlorate or other chaotropes and will repolymerize in vitro to form milligram amounts of wall crystals. Conditions for optimal crystalization are presented, and conditions that fail to induce polymerization are exploited to maintain monomers in aqueous solution for ion-exchange chromatography. The four major glycoproteins of the complex (GP1, 1.5, 2, and 3) have in this way been purified to apparent homogeneity and have been characterized morphologically by transmission electron microscopy using the quick-freeze, deep-etch technique and by amino acid composition. Three of the four are hydroxyproline-rich species that copolymerize to form the W6 layer. The fourth (GP1.5) is a glycine-rich species that binds to the interior of the in vitro crystal; it is apparently equivalent to the granules within the W4 layer in situ.

THE extracellular matrices of both plant and animal cells are, by definition, assembled extracellularly, meaning that all the information necessary for the ultimate form of a given matrix is contained within its component proteins and polysaccharides. In some cases, the best studied being type I collagen (2), the matrix protein is secreted as a precursor that can only assemble after being processed by extracellular enzymes; in other cases (9, 14), the patterning of the matrix appears to be accomplished, at least in part, by the sequential secretion of different components. Much experimental evidence (34) indicates that cellular differentiation is often accompanied, or predicted, by alterations in the extracellular matrix, and that the dedifferentiation events that accompany malignant transformation can include matrix alterations (5). Therefore, an understanding of matrix assembly has widespread implications.

We have chosen to study the assembly of the extracellular matrix of *Chlamydomonas reinhardtii*, a unicellular eukaryote, because it offers unique advantages as an experimental system. (*a*) The matrix is highly organized and invariant, and several of its layers are fundamentally two-dimensional (31), permitting analysis of its organization that becomes far more difficult with three-dimensional arrays. (*b*) Two of the layers can be disassembled using chaotropic agents and will reassemble in vitro when the chaotropes are removed (13, 17), permitting critical analysis of the assembly process by methods used, for example, in studies of collagen (2). (*c*) The glycoproteins that make up the matrix are fibrous hydroxyproline-rich species that are likely to be evolutionary homologues of the major matrix proteins of higher plants (21, 30), and are at least analogues of the hydroxyproline-containing collagens of higher animals; therefore, information about their assembly promises to increase our understanding of multicellular interactions.

In a previous paper (13), we described the overall architecture of the *Chlamydomonas* cell wall as visualized using the quick-freeze, deep-etch technique (15), which provides unparalleled views of its fibrous organization and its component glycoproteins. In the present study we have focused on the in vitro assembly and disassembly of the W6 and W4 layers of this wall, extending a system first developed by Roberts and his colleagues (17). We go on to describe the purification, morphology, and amino acid composition of each of the four major glycoproteins that assemble into these in vitro crystals, and discuss the evolutionary and functional implications of our findings.

Materials and Methods

Crystal Formation

A general protocol for generating wall crystals from the *bald-2* strain of *C. reinhardtii* is provided in reference 13; details are as follows. After harvesting a 5-l culture of vegetatively grown *bald-2*, the cell pellets are washed twice in two 200-ml vol of distilled water. The second pellet is suspended in ~80 ml water, divided between two 50-ml tubes, and pelleted at 17,000 *g* for 4 min. The supernatant is decanted and the packed volume of each pellet is estimated. A volume of 2 M sodium perchlorate (Sigma Chemical Co., St. Louis, MO) in water equivalent to the packed cell volume is mixed with the pellet, and the suspension is allowed to sit at room temperature for 20 min with occasional gentle agitation. This treatment kills the cells but does not result in any cell lysis. The bulk of the cells are then pelleted at 3,000 *g*

for 2 min, and the supernatant is centrifuged at 40,000 *g* for 10 min to pellet any remaining cells and extracted wall "shells" (13). This supernatant, typically ~40 ml, is placed in 1-in. dialysis tubing and dialyzed overnight at room temperature against 6 liters of distilled water containing 0.02% sodium azide. During the course of the next day the dialysis water is changed two more times. A cloudy precipitate sometimes forms during this time. Towards the end of the second day the dialyzed material is transferred to two 250-ml beakers and rapidly frozen by placing the beakers at the bottom of a −70°C freezer. The beaker contents are then lyophilized to dryness, yielding two fluffy, pure white primary lyophilates. These are combined and suspended in 5 ml 1 M sodium perchlorate, with vigorous pipetting over a 15-min period to break up the lyophilate and effect its maximal solubilization. By phase microscopy, the salt-insoluble material remaining in this suspension appears as granular aggregates; by electron microscopy it has the form of tangled long fibers; when boiled in SDS/β-mercaptoethanol (β-Me)[1] lysis buffer, it forms an insoluble residue and yields no bands when subjected to SDS PAGE (not shown). We suspect that this material derives, at least in part, from the outermost W7 layer of the wall, which consists of long anastomosing fibers (13), but we have not analyzed it further. The salt-insoluble material is pelleted at 40,000 *g* for 10 min, and the supernatant dialyzed against 4 liters of water plus 0.02% azide overnight to yield abundant white crystals suspended in a crystal supernatant. Typical dry weight yields per 5-liter culture are 110 mg primary lyophilate, 25 mg salt-insoluble material, 25 mg crystals, and 30 mg crystal supernatant. The unrecovered material presumably adsorbs to dialysis tubing and glassware since, to maximize protein concentration, these vessels are not rinsed.

Purification and Analysis of Crystal Glycoproteins

As starting material for crystal glycoprotein purification, we used either crystal supernatants (see above) or crystals (~25 mg) dissolved in 20 ml 1 M sodium perchlorate and then dialyzed overnight against water; as described in Results, the glycoproteins fail to crystalize overnight at such dilutions and therefore remain in solution in water.

Glycoproteins (GP) 1, 2, and 3 were purified using an analytical MonoS cation-exchange column (Pharmacia Inc., Piscataway, NJ) and a high-pressure liquid chromatography system consisting of two M-6000A pumps (Waters Instruments, Inc., Rochester, MN), a V7 valve and mixer (Pharmacia Inc.), a 785 chrome ultraviolet monitor (Micromeritics Instrument Corp., Norcross, GA), a 720 system controller (Waters Instruments Inc.), a Frac-100 fraction collector (Pharmacia Inc.) operating in the peak-cutting mode, and an IBM 9000 computer and associated chromatographic software (IBM Instruments, Inc., IBM Corp., Danbury, CT). Absorbancies were monitored at 280 nm. The MonoS column was equilibrated with a 50 mM potassium acetate buffer, pH 5.5. The aqueous glycoprotein solution was loaded using a 50 ml Superloop (Pharmacia Inc.) at 1.5–2 ml/min. Proteins were then eluted using a linear 0–500 mM gradient of KCl in the acetate buffer, applied over a 15-min period with a flow rate of 1.5 ml/min; the salt concentration was then raised abruptly to 1 M KCl for an additional 3 min.

GP1.5 fails to adsorb to the MonoS column and appears in the flow-through. This flow-through was conserved and loaded onto a MonoQ analytical anion-exchange column (Pharmacia Inc.) equilibrated with 20 mM Hepes buffer, pH 7.4. Using the same high-pressure liquid chromatography system described above, protein was eluted from this column using a linear 0–500 mM KCl gradient in the Hepes buffer applied over 15 min, followed by a 3-min elution using 1 M KCl. The GP1.5 protein elutes with the 1 M KCl front.

Fractions from both columns were dialyzed overnight against water and lyophilized to dryness. For SDS PAGE of these fractions and of the starting crystals and supernatants, samples were brought up in lysis buffer, with or without 10% β-Me, boiled (ordinarily) for 3 min, and analyzed using a 5–15% gel gradient as described in reference 1. Gels were initially stained using the periodic acid–Schiff (PAS) reagent as described in reference 24. In some cases they were washed and counterstained with silver using the method of Morrissey (25) to ascertain that additional PAS-negative polypeptides were not present (c.f. reference 13).

Amino acid analysis was performed by bringing up lyophilates of purified glycoproteins in 6 M HCl and boiling for 18 h at 105°C. The hydrolysates were dried with a Speed-Vac concentrator and resuspended in amino acid analyzer buffer (Pierce Chemical Co., Rockford, IL). Amino acid composition was determined using a Beckman 119 C amino acid analyzer (Beckman Instruments, Inc., Palo Alto, CA) as described by Mecham and Lange (23). Cysteine was measured as cysteic acid after performic acid oxidation. Samples were also examined for amino-sugar residues, but none were detected.

Quick-freeze, deep-etch electron microscopy of crystals was performed as described in Heuser (15); glycoproteins adsorbed to mica flakes were prepared and visualized as described in Heuser (16) and Goodenough and Heuser (12).

Results

Wall Crystal Preparations

The cell wall of *Chlamydomonas* contains a single crystalline layer, designated W6; Catt et al. (4) concluded that layer W2 is also crystalline, a conclusion we believe to have been erroneous (see Discussion). In our previous study (13) we analyzed the structure of W6 in intact walls and in isolated walls that had been homogenized to release W6 from underlying layers, and concluded that the crystal is composed of two ordered subdomains, a tightly woven inner W6A and a loosely woven outer W6B.

The present study focuses on an additional type of W6 crystal preparation that was briefly described in our previous article (13). A detailed protocol is provided in Materials and Methods. In brief, living cells are suspended in 1 M sodium perchlorate, which strips them of their W6 and W4 wall layers (13) but, remarkably, causes no cell lysis. When the perchlorate-soluble material is dialyzed against water, an abundant yield (~25 mg) of large (>10 μm) crystals is obtained which, by phase microscopy (Fig. 1), are seen to stack on top of one another. By quick-freeze, deep-etch electron microscopy (Fig. 2), each crystal in the stack is found to consist of two layers bridged by an array of granules, equivalent to the double-layered structures visualized by Catt et al. (reference 4, Fig. 6 *d*) in preparations derived from isolated cell walls.

Fig. 3 is a diagram of our hypothesis of how such structures are generated. We propose that perchlorate releases both W6 material and the granular constituents of the W4 layer, and that during dialysis, two W6 layers come to be conjoined, with W4 granules in the interior of the "sandwich."

Figs. 4 and 5 show the kinds of images that have led to this model. In Fig. 4, a sandwich is viewed from above, and the tightly woven structure of its upper surface is clearly similar to the W6 layer of the in situ wall (13). This surface has been partially fractured away to reveal the granular interior of the sandwich, which contains fibrous strands and prominent granules. Since the granules are sufficiently similar in size and disposition to the granules found in the W4 layer of the in situ wall (reference 13; Figs. 2, 4, and 7), we shall equate the two here, although we stress that this identity has not yet been proven. In Fig. 5, a sandwich adsorbed to a mica flake by its lower surface has been fractured tangentially. According to the model drawn in Fig. 3, the uppermost and lowermost surfaces of the sandwich should carry the W6B open weave. Elements of this weave on the upper surface are indicated by large arrowheads. At the lower surface, the mica has induced the weave to depolymerize into a collection of long fibrous proteins (arrow) equivalent to the 100-nm fibers described previously (13). Therefore, as speculated in reference 13, the 100-nm fibers assemble to form the W6B weave (their pattern of assembly will be the subject of a separate report.[2]

1. *Abbreviations used in this paper*: β-Me, β-mercaptoethanol; GP, glycoprotein; PAS, periodic acid–Schiff.

2. Goodenough, U. W., and J. E. Heuser. Manuscript in preparation.

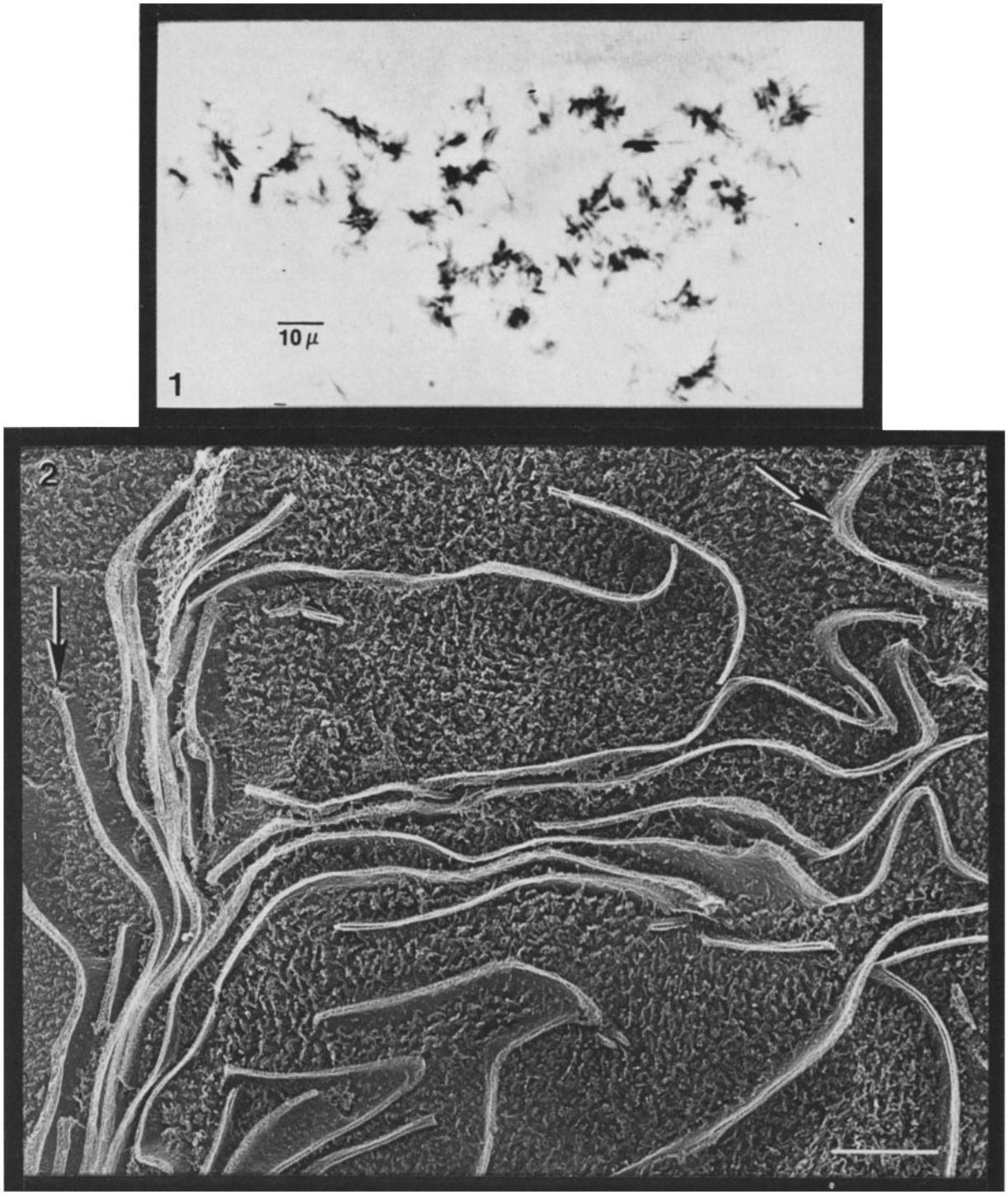

Figures 1 and 2. (Fig. 1) Crystal aggregates visualized by phase microscopy. Bar, 10 μm. (Fig. 2) Portion of a crystal aggregate visualized by quick-freeze, deep-etch electron microscopy. Arrows indicate regions where the lamellae can be resolved as two leaflets bridged by granular elements. Bar, 1 μm.

Above the depolymerized 100-nm fibers in Fig. 5, the fracture reveals a portion of the inner aspect of the lower layer, which displays a periodic beaded substructure. Small arrowheads delineate one of the 28 × 24-nm parallelograms that constitute the unit cell of this crystal, and its configuration is identical to the units found on the inner surface of the W6A layer in the in situ wall (13, 28).

Concentration Dependence of Crystal Formation

Hills et al. (17) note that when they dialyzed whole-wall perchlorate-soluble fractions against water, only 40% (wt/wt) of the material was recovered as pelletable fragments, even though they state that the remaining material is electrophoretically identical to what is incorporated into the fragments. Fig. 6 compares gel profiles of original perchlorate-

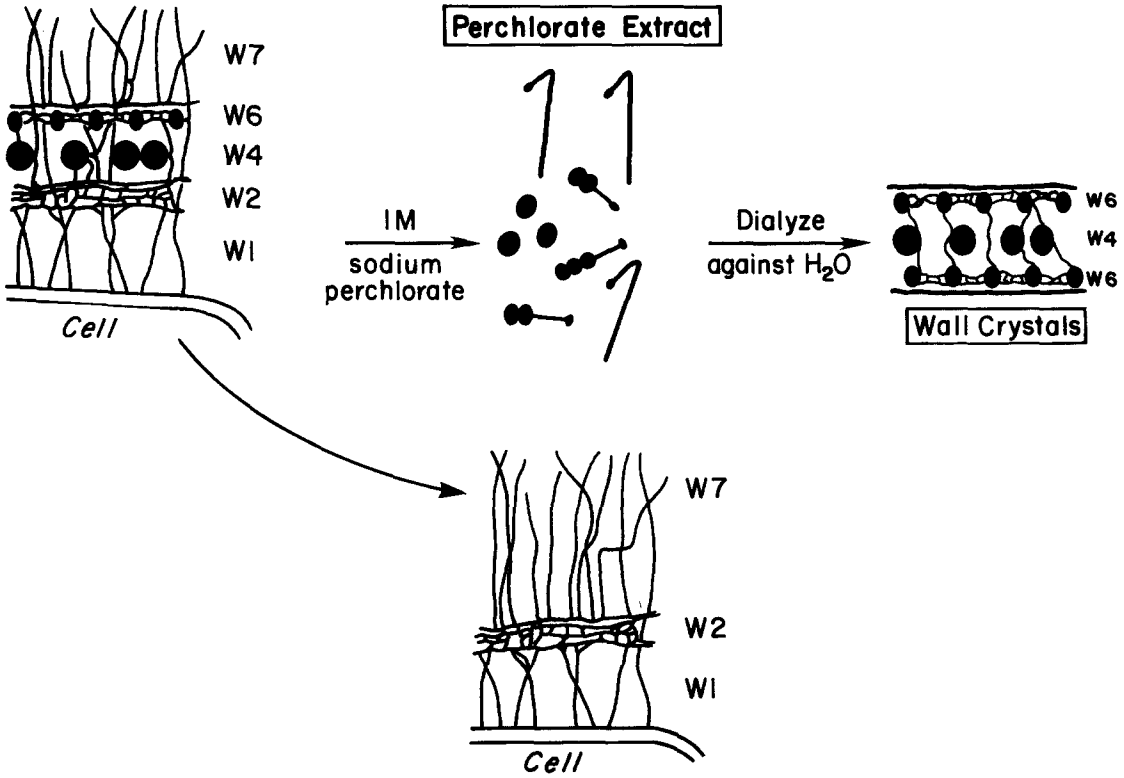

Figure 3. Diagram of the postulated sequence of events in wall crystal formation in vitro.

soluble material (primary lyophilate) (lane *A*), crystals formed after water dialysis (lane *B*), and the nonincorporated "crystal supernatant" material (lane *C*). The crystals and crystal supernatants are in fact not electrophoretically identical: the bands labeled 4 and 5, present in the original extract (lane *A*), are not incorporated into the crystal (lane *B*) and remain in the supernatant (lane *C*). While this could simply mean that bands 4 and 5 are perchlorate-soluble glycopolypeptides that fail to become part of the crystal (at least in vitro), it could also mean that bands 4 and 5 are inhibitors of crystal formation (e.g., proteolytic fragments of native glycoproteins), their presence explaining why a certain proportion of the solubilized glycopolypeptides fail to crystalize.

Additional experiments have indicated that the glycoproteins in the crystal supernatants in fact fail to polymerize because they are too dilute, and not because bands 4 and 5 are inhibitors. Thus in a typical experiment in which 87 mg of a primary lyophilate was solubilized in 5 ml of perchlorate, 26 mg of protein (dry wt) proceeded to form crystals upon overnight dialysis, while 30 mg (dry wt) remained in the supernatant (% recovery of material in these experiments is low because dialysis tubing and glassware are not rinsed to avoid further dilution of the sample). If the lyophilized crystal supernatant is solubilized in another 5 ml of perchlorate and dialyzed overnight, no crystals will form, whereas if it is instead solubilized in only 1 ml of perchlorate, it will yield ~5 mg (dry wt) of crystals, with the remainder of the protein again in a second "crystal supernatant." SDS PAGE documents that the second 5 mg of crystals contain the same glycopolypeptides as the first 26 mg (that is, the Fig. 6, lane *B* pattern), and that the second crystal supernatant continues to retain bands 4 and 5. Thus the presence of glycopolypeptides 4 and 5 in the solution does not prevent crystal formation per se, whereas suspending the glycoproteins at too great a dilution does prevent crystal formation.

The same conclusion is reached when the experiment is performed as follows. A primary lyophilate (114 mg dry wt) was divided in half; sample A (56 mg) was suspended in 20 ml perchlorate, and sample B (58 mg) in 5 ml perchlorate. Undissolved material was pelleted (~11 mg each sample), and each supernatant was dialyzed overnight against water. In sample A, only 0.35 mg of crystals formed, with 43 mg (dry wt) remaining in the supernatant, whereas in sample B, 12 mg of crystals formed, with only 20 mg (dry wt) remaining in the crystal supernatant. It is clear, therefore, that crystalization under these conditions requires a critical concentration of unpolymerized monomer. (We should note that all these experiments use an overnight dialysis. If dialyzed crystal supernatants are allowed to stand for longer periods, crystals continue to form at a slow rate, indicating, not surprisingly, that crystalization depends on both monomer concentration and time).

We have taken advantage of the above observations to frac-

Figures 4 and 5. (Fig. 4) Double-layered crystal absorbed to mica, viewed from above. A large area of the W6 tight weave has been fractured to reveal an internal domain of W4 granules. Bar, 200 nm. (Fig. 5) Double-layered crystal viewed in tangential fracture. The upper W6B layer carries an open fibrous meshwork (*large arrowheads*); comparable fibrous components of the lower W6B layer have depolymerized on the mica surface (*arrow*). The inner surface of the lower W6A layer carries the diagnostic crystal unit indicated by the four small arrowheads. Bar, 100 nm.

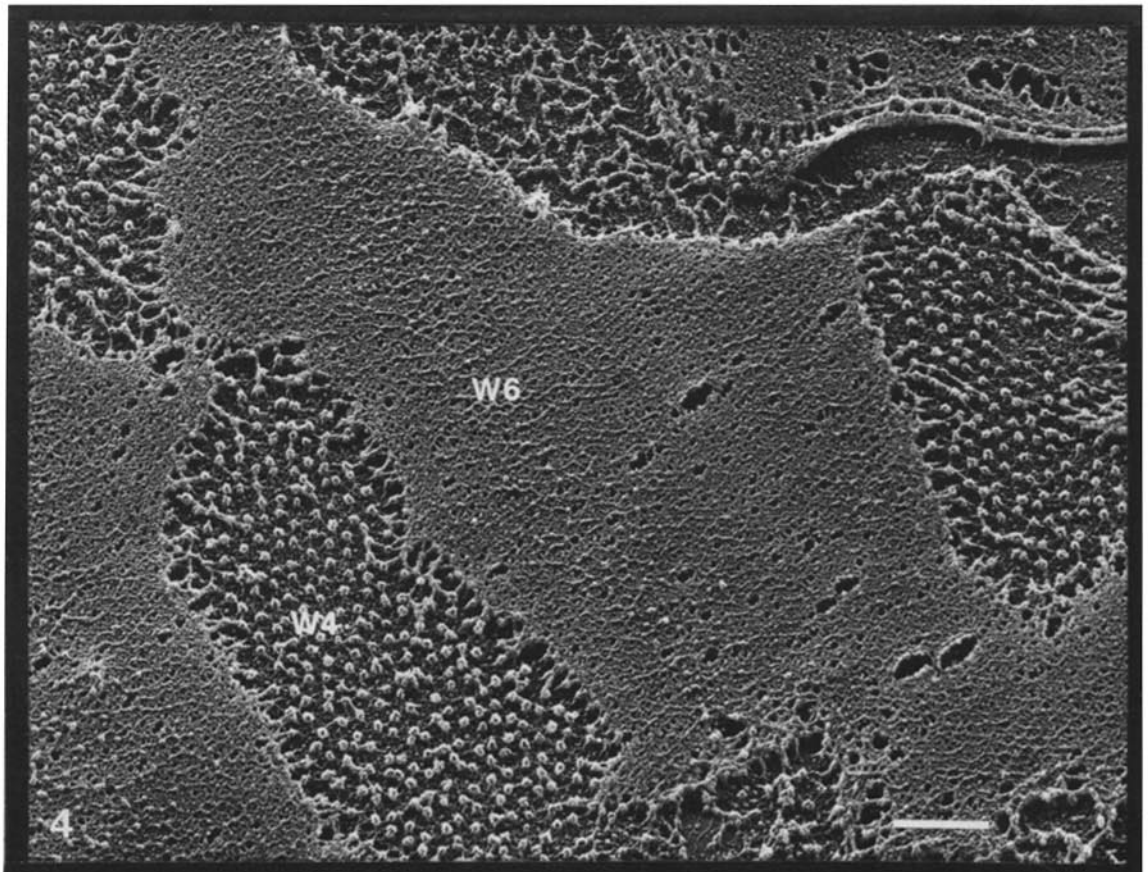
W6
W4
4

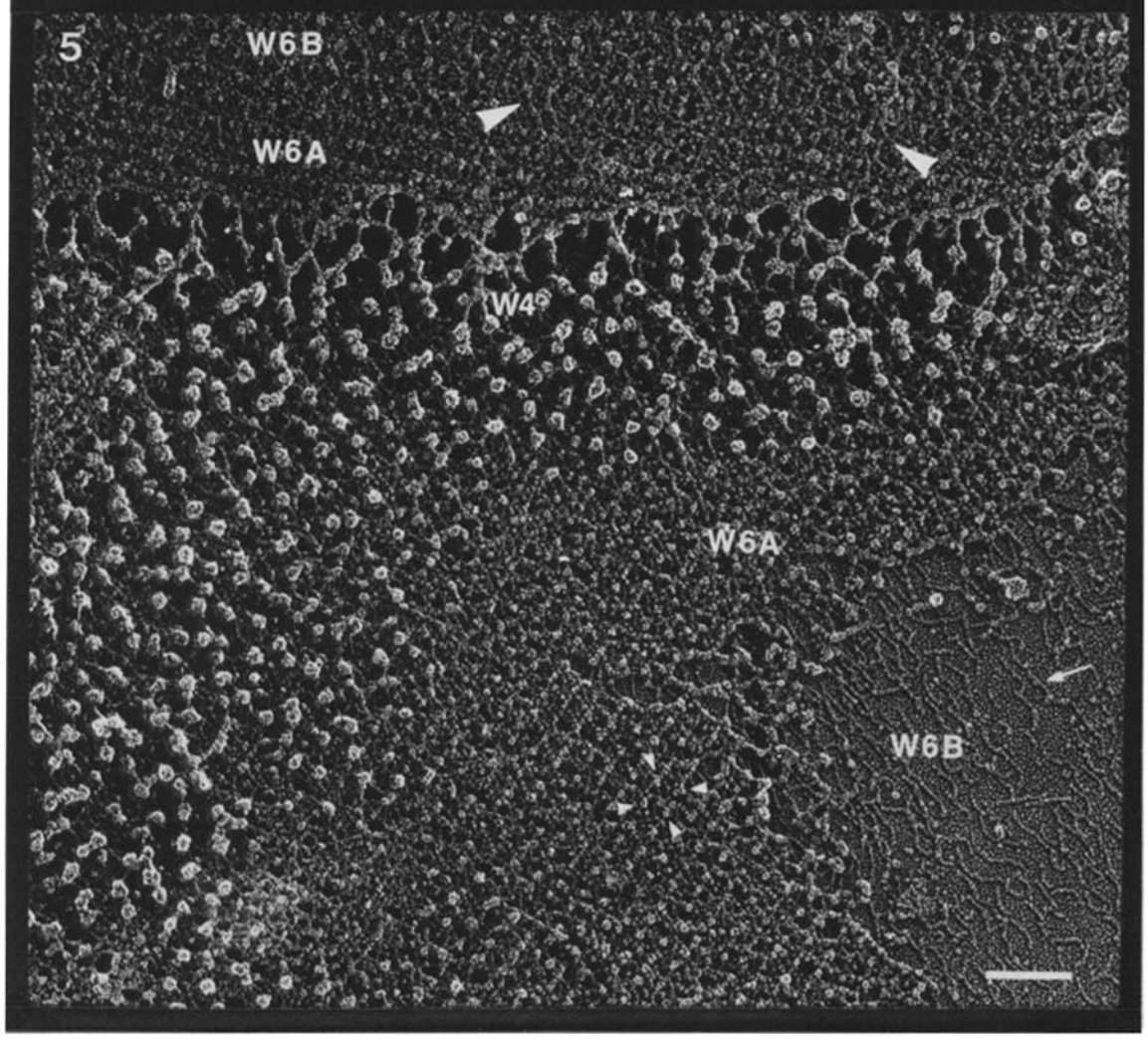
5
W6B
W6A
W4
W6A
W6B

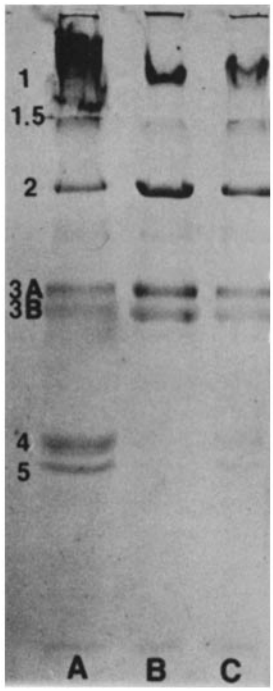

Figure 6. PAS-stained SDS PAGE of a primary lyophilate (*A*), a crystal preparation (*B*), and a crystal supernatant (*C*). Bands *4* and *5* are absent from the crystals.

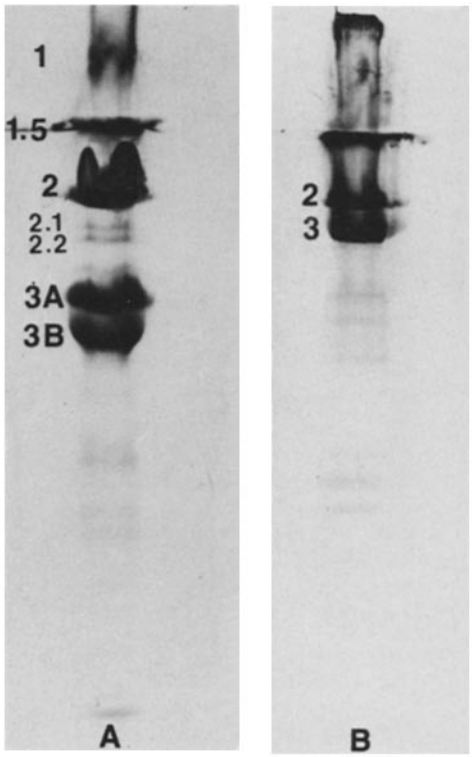

Figure 7. PAS-stained SDS PAGE of crystals solubilized in the presence (*A*) or the absence (*B*) of 10% β-Me and 100°C exposure.

tionate the wall components on ion-exchange columns. As long as crystal proteins are dissolved in 1 M sodium perchlorate, ion-exchange columns cannot be used, and attempts to fractionate the proteins by gel filtration in the presence of perchlorate have yielded mixtures of the starting proteins rather than individual species (e.g., the 2BII fractions described in references 3 and 4). We have instead used as starting materials either the "crystal supernatants" described above, or else crystals dissolved in a volume of perchlorate so large that crystals will not form when the solution is dialyzed overnight against water. Thus, by working with wall components below their critical concentration, we can keep them in aqueous solution, load them onto ion-exchange columns, and purify each species to homogeneity (see later sections).

Solubility of the Chlamydomonas Crystals

Roberts and co-workers reported three salt solutions (5 M CsCl, 1 M $NaClO_4$, and 8 M LiCl) that would dissolve cell wall crystals, with LiCl and CsCl being at least partially denaturing (17). We carried out additional studies of this kind to glean more information on the kinds of chemical interactions that stabilize the lattice. The crystals prove to be stable to 250 mM EDTA and to 10% deoxycholate. They are solubilized by 1 M urea (in 100 mM Tris) and by 200 mM dithiothreitol, but in both cases fail to reassemble after overnight dialysis, suggesting that these reagents have a denaturing effect on one or more of the crystal components. Finally, they are dissociated by chaotropic agents in the Hoffmeister series at neutral pH. KI is the most potent, dissociating at 125 mM; NaBr is the least potent, dissociating only at 1 M; and the range is as follows: $I^- > NO_3^-$ = guanidinium > $SCN^- > Cl^- > ClO_4^- > Br^-$. Walls solubilized in buffered 250 mM KI reassemble upon water dialysis as well as 1 M perchlorate-solubilized walls, and the relatively low KI concentrations required indicate that it is the solubilizing reagent of choice. We have, however, used perchlorate throughout this series of experiments to permit direct comparisons with the earlier studies of Roberts and collaborators.

Electrophoretic Characterization of the Crystal Glycopolypeptides

By SDS PAGE in the presence of 10% β-Me, the crystals display four major glycopolypeptides, labeled 1, 2, 3A, and 3B in Fig. 6 *B*,[3] in roughly equivalent proportions. It is not possible, however, to deduce exact stoichiometries from such gel data since glycopolypeptides may stain anomalously by either the PAS or the silver technique. Moreover, band 1, which migrates only partially into the stacking gel, often fails to form a sharp band (e.g., Fig. 7 *A*), making it difficult to quantitate.

The band labeled 1.5 in Figs. 6 and 7 stains a characteristic magenta color with the PAS reagent. The amount of this species varies considerably from one crystal preparation to the next, being barely detectable in some samples (Fig. 6 *B*) and prominent in others (Fig. 7 *A*). It migrates only to the stacking gel/running gel interface and, in heavily loaded gels, proceeds to migrate laterally along this discontinuity (Fig. 7 *A*).

3. In a previous article from this laboratory (24), cell walls were labeled in situ with ^{125}I and analyzed by SDS PAGE/autoradiography. Unfortunately, material migrating in the stacker gel was not included in this analysis, so that bands 1 and 1.5 were not included in the resultant catalogue. We are therefore offering a new numbering system here to denote perchlorate-soluble glycopolypeptides detectable by PAS staining. Bands W1, W6, and W7 in the Monk et al. (24) catalogue correspond to bands 2, 3A, and 3B in the present system. They have been shown to migrate as 280-, 165-, and 140-kD species (24).

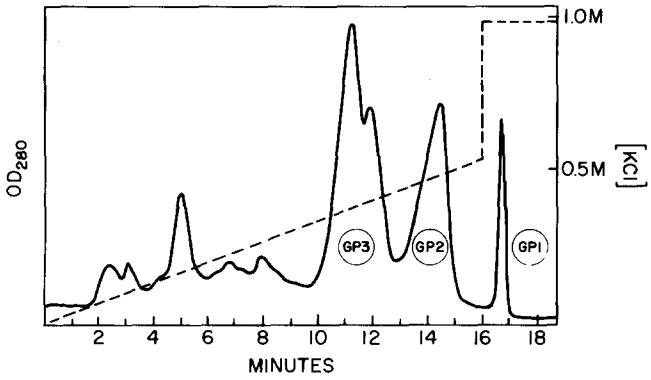

Figure 8. Chromatographic profile of GP3, GP2, and GP1 elution from a MonoS cation-exchange column, where starting material was a crystal supernatant.

When β-Me is omitted from the SDS lysis buffer and the sample is not boiled, a new band, labeled 3 in Fig. 7 *B*, is prominent in SDS gels and bands 3A and 3B are absent. These results suggest that 3A and 3B are held together by disulfide bridges. Curiously, however, if β-Me is rigorously omitted from the system (careful washing of gel rigs, use of fresh plasticware, etc.) and samples dissolved in SDS are simply boiled, most of band 3 is also found as 3A + 3B. When β-Me is present, by contrast, no boiling is required to dissociate the protein (data not shown). Therefore, the β-Me-sensitive linkages are also heat-labile, indicating that they are not classic disulfide bonds.

Two additional glycopolypeptides in the crystal, labeled 2.1 and 2.2 in Fig. 7 *A*, are minor components that are always present in equivalent amounts. Additional glycopolypeptides migrating ahead of band 3B are also present in variable trace amounts.

Purification and Properties of Four Crystal Glycoproteins

Using ion-exchange chromatography, it has been possible to obtain fractions containing only bands 1, 2, 3A + 3B (or 3 in the absence of β-Me and heat), and 1.5. We therefore conclude that each fraction contains an independent glycoprotein, which we hereafter designate as GP1, GP2, GP3, and GP1.5. Fig. 8 shows the elution profile from a cation-exchange column, which separates GP1, GP2, and GP3; GP1.5 flows through this column and is retained on an anion-exchange column. SDS PAGE of the purified proteins is shown in Fig. 9, and Figs. 10–13 show the morphology of each purified protein by quick-freeze, deep-etch electron microscopy. A mixture of GP1, GP2, and GP3 is shown in stereo in Fig. 14 to indicate the three-dimensional topology of each protein, and a summary of the molecular dimensions of each species is given in Table I.

The GP1 species (Fig. 10) proves to be the fibrous 100-nm component of the crystal that we (13) and Roberts (28) recognized earlier in monomer mixtures. This assembles into the W6B weave (Fig. 5). It carries a globular head and often displays bends or kinks at two characteristic positions along its fibrous shaft (designated a and b in Fig. 10; see also Table I). It has a high affinity for the mica surface—it is the predominant absorbed protein when an unfractionated perchlorate extract is mixed with mica flakes, even though it

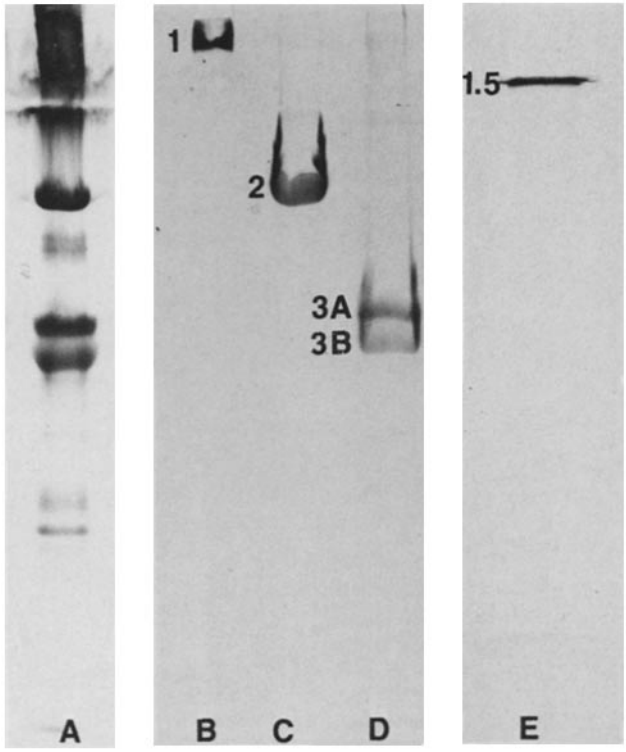

Figure 9. PAS-stained SDS PAGE of starting crystal supernatant material (*A*), purified GP1 (*B*), GP2 (*C*), GP3 (*D*), and GP1.5 (*E*).

represents only ~⅓ of the total protein in such a sample (Fig. 6). It also tends to align along one crystallographic plane on the mica (Figs. 10 and 14). The kink at position a (the "major kink") is more likely to persist during the alignment process than is b (the "minor kink"), but the shaft may also straighten out completely (Fig. 10, row 4).

The GP2 and GP3 species, which co-polymerize to form the dense W6A layer,[2] were lumped together under the term "elongated globular elements" in our previous report (13), and indeed they are very similar in structure. Each carries a small terminal head, indistinguishable from that found on GP1; behind the head is a short fibrous domain we designate the neck; and behind the neck are several larger globular domains that constitute the body. The GP2 body consists of two discrete globular domains, whereas GP3 carries three poorly defined domains that often merge into one another. In mixed

Table I. Dimensions of the Four Glycoproteins Purified from Wall Crystals

Protein	Map	Head	A	B	C	Total length
		nm	*nm*	*nm*	*nm*	*nm*
GP1		7	28	42	30	100
GP2		7	25	12		46
GP3		7	28	10	10	56
GP1.5	○					14

At least 10 proteins were measured at 680,000 × and average lengths were calculated for the intervals designated on the protein maps. Head measurement represents the average of the longer dimension (the heads are slightly ellipsoidal).

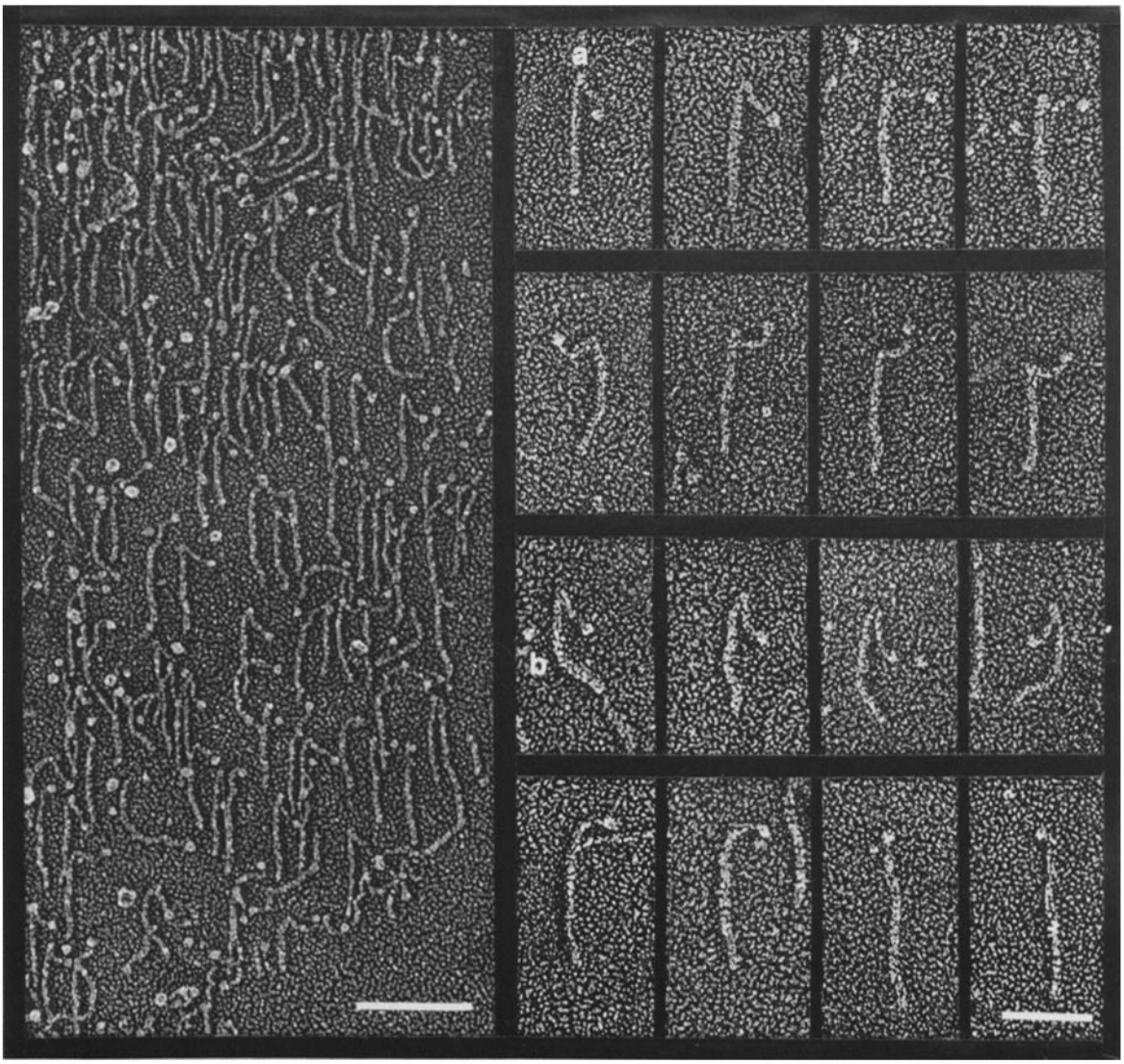

Figure 10. GP1 proteins. (*Left*) Field of purified proteins. Bar, 100 nm. (*Right*) Montage of single proteins. Rows 1 and 2 show kinks at site *a*. Row 3 shows kinks at sites *a* and *b*. Row 4 shows molecules with bends at site *a* or with no kinks. Bar, 50 nm.

populations derived from depolymerized crystals (Fig. 14), GP2 and GP3 tend to align at right angles to GP1, a phenomenon first noted in our previous study (13). In such mixtures, GP2 and GP3 are best distinguished from one another by their characteristic mode of mica adsorption: the head and neck of GP2 tend to lie on the mica surface at right angles to the body, like a swan on a pond, whereas the head and neck of GP3 are more parallel to the body, like a swan in flight. These same two configurations are found if the proteins are fixed in 0.1% glutaraldehyde before mica adsorption; therefore, either glutaraldehyde induces the same morphologies as the mica surface or, more likely, the two configurations are true to the native proteins.

The relatively large range in the dimensions of both GP2 and GP3 (Figs. 12 and 13) reflects, we believe, different degrees of distortion incurred as individual molecules adsorb to mica. Thus some proteins appear quite compact, with the body domains standing high off the mica surface when viewed in stereo (Fig. 14), whereas others appear strung out, with relatively flat body domains (as noted above, this tendency is more pronounced for GP3 than for GP2). It would be logical to assume that the more flattened images reflect more severe levels of adsorption-induced denaturation; if, however, the proteins are relatively hydrophobic, then the compact image may be generated by a relative aversion of some parts of the molecule to the charged mica surface.

The GP1.5 species proves to be unique among the four in that it displays no fibrous domains and is selectively retained on an anion-exchange column. Because salt crystallites on mica are often of similar dimensions, it is difficult to identify GP1.5 unambiguously in a mixed monomer preparation (Fig. 14); when purified, however, its homogeneous size (14 nm) is diagnostic (Fig. 13). GP1.5 appears morphologically identical to the globular material within the crystal sandwiches (Figs. 4 and 5), material similar in structure to the in situ W4 granules (13).

Table II shows the amino acid composition of the four glycoprotein species. The following features of the data are of

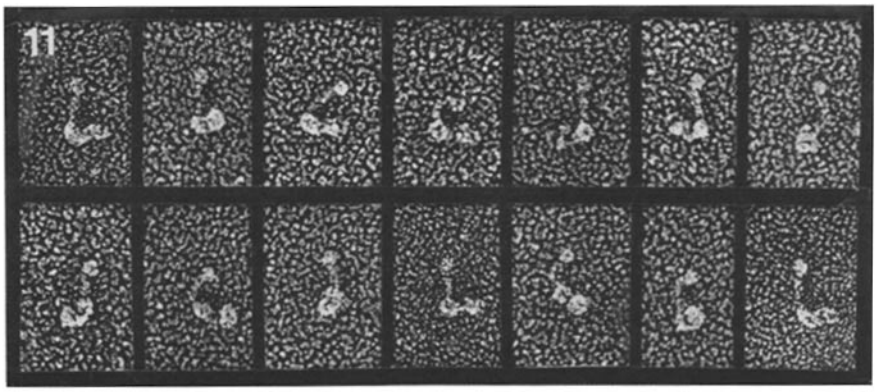

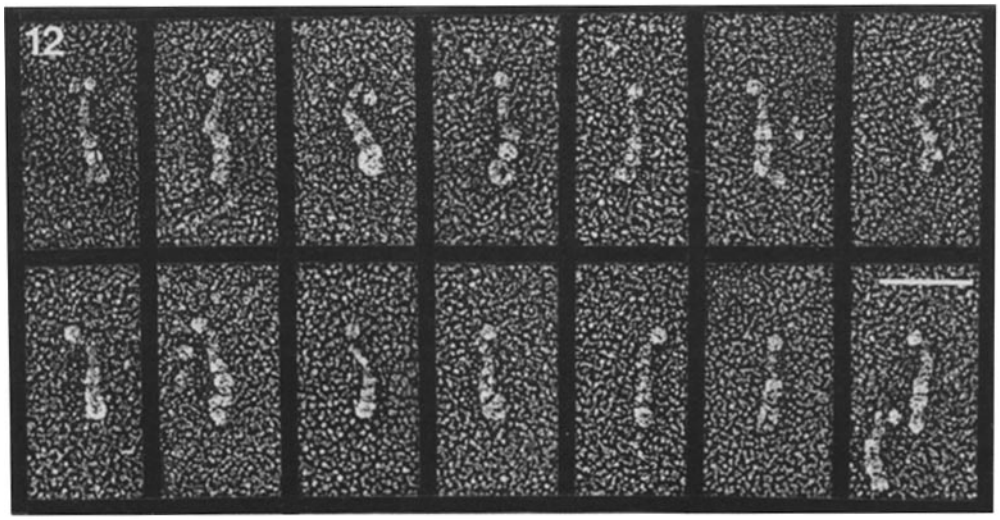

Figures 11 and 12. (Fig. 11) GP2 proteins. The small head points upward, borne by a narrow neck; the bipartite body may condense to form a more compact unit. (Fig. 12) GP3 proteins. The small head is at the top of each molecule, beneath which a neck melds into the three indistinct domains of the body. Bar, 50 nm.

interest. (*a*) The high hydroxyproline content (32%) of GP1 is consonant with its fibrous structure, suggesting that much of the protein may be in the form of an extended polyproline helix (18, 21). Conversely, the low (1.5%) hydroxyproline content of GP1.5 is consonant with its globular structure. Indeed, since GP1.5 displays no fibrous domains, this 1.5% possibly reflects the level of contamination of the sample with other hydroxyproline-rich proteins. (*b*) GP2 and GP3, which are similar in structure, have similar amino acid compositions in most cases, but there are noteworthy differences. Thus GP2 has significantly more tyrosine and less isoleucine and histidine than has GP3. Moreover, GP2 has almost three times the hydroxyproline of GP3, even though both proteins have similar fibrous domains (Figs. 12 and 13), and its ratio of hydroxyproline to proline is much larger. Finally, GP3 has more than three times as much cysteine as GP2, presumably reflecting its lability to reducing agents (Fig. 7). (*c*) GP1.5 has remarkably high levels of glycine (23%) and contains 24% acidic amino acids, presumably explaining its high affinity for anion-exchange resins.

Sepharose 2BI Material

Catt et al. (4) report that when a cell wall perchlorate extract is fractionated over Sepharose 2B, they detect two major peaks, an early-eluting 2BI and a later-eluting 2BII, with the 2BII fraction alone capable of forming crystals upon dialysis. Fig. 15 *A* shows the glycopolypeptide composition of these two fractions as analyzed by our SDS PAGE system. The profile is identical to that reported by Catt et al. (4) except that the 2BI material, which fails to enter their 5% gels, produces a broad smear in our 3% stacking gel (and accounts for the smearing of the stackers of Figs. 6 *A* and 9 *A*). Note that the 2BI component is present in the 2BII fraction, which appears also to be the case in the Catt et al. study (4).

The 2BI material proves also to be the major component present in the crystal supernatant fractions that elute early from our MonoS columns (Fig. 8). When these fractions are analyzed individually or pooled, their SDS PAGE profile (Fig. 15 *B*) again shows a broad PAS-positive smear in the stacker region.

Fig. 15 *C* shows a quick-freeze, deep-etch view of this material from a 2BI fraction. It consists of delicate fibrils, of indeterminate length, which aggregate into clots. By amino acid analysis (4), the 2BI fraction has been shown to be rich in hydroxyproline (11%), yet the loose, meandering appearance of these fibrils is very different from the stout, rigid fibrillar domains of the crystal glycoproteins.

Taken together, the 2BI material appears to be a perchlorate-soluble hydroxyproline-rich component of the wall which is not included in in vitro crystals. We have not assessed its reported ability (4) to increase the size of in vitro

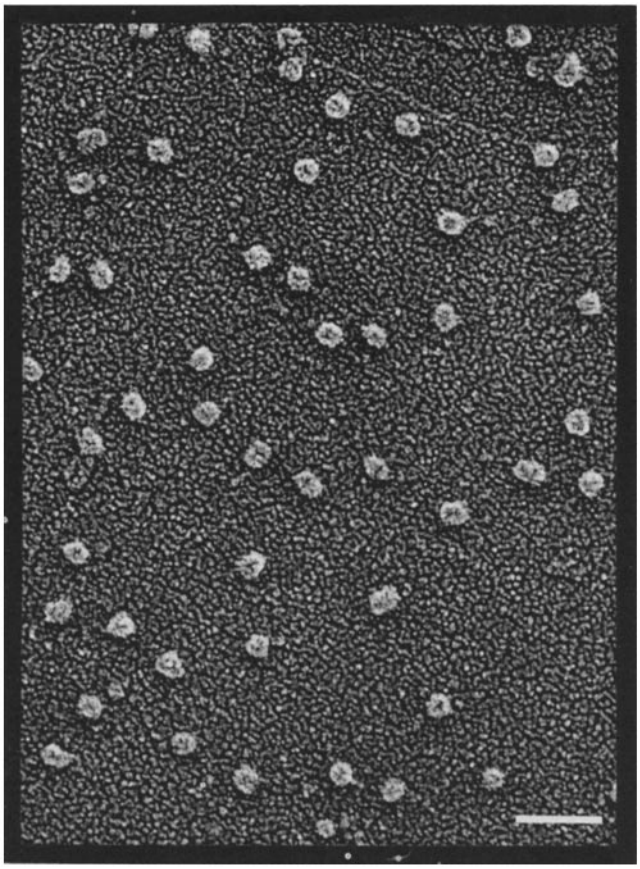

Figure 13. GP1.5 proteins. Bar, 50 nm.

crystals, nor has the cell wall layer from which it derives been determined.

Discussion

Wall Crystal Organization

The in situ cell wall of *Chlamydomonas* is a seven-layered structure with three conspicuous layers, W2, W4, and W6 (separated by spaces W3 and W5) that make up the "central triplet" (31). In their original study, Roberts et al. (31) concluded that each layer of the central triplet was different in structure and that only the outermost layer (W6) displayed a crystalline order. In later studies, however, they concluded that W2 is also crystalline and identical in structure to W6 (4).

In our recent deep-etch analysis of the in situ wall (13), we confirmed the original conclusion of Roberts et al. (31), documenting that the W2 domain is an anastomosing network of fibers and that only W6 shows crystalline periodicity. To explain their subsequent reinterpretation, we propose the following. As diagrammed in Fig. 3 and documented in our earlier report (13), perchlorate releases W6 and W4 material from the wall, leaving behind the insoluble W2 (see also references 19 and 22). Upon dialysis, this salt-soluble material forms W6-W4-W6 sandwiches (Figs. 2–5). Catt et al. (4) produced thin-section images of such in vitro sandwiches (their Fig. 6 *d*), and then detected identical structures near the surface of living cells (their Fig. 6 *a*), leading them to propose that the inner W2 layer is in fact a duplicate of the outer W6. We suspect, however, that during the prolonged culture conditions used in their studies, some proportion of the cell walls released at each mitosis first dissociated into W6-W4 units and then either folded on themselves or associated laterally to form W6-W4-W6 sandwiches, as in Fig. 3. Some of these sandwiches, we further propose, adhered to the outer surfaces of cells to create the impression that they were true in situ walls.

Concentration Dependence of Crystal Formation

Using unfractionated perchlorate extracts, we find that crystal size is invariably large (>10 μm) and quite uniform, but that crystal abundance is highly dependent on concentration of unpolymerized monomer. Thus, for example, the same dry weight of monomer (~50 mg) will generate ~12 mg of crystals when suspended at ~10 mg/ml but <1 mg of crystals when suspended at ~2 mg/ml, the remaining unpolymerized protein forming a "crystal supernatant" which is competent to form more crystals if lyophilized and resuspended at higher concentrations or allowed to crystallize for longer time periods. This concentration dependence may bear on the mechanism of crystal formation in vivo. We have shown

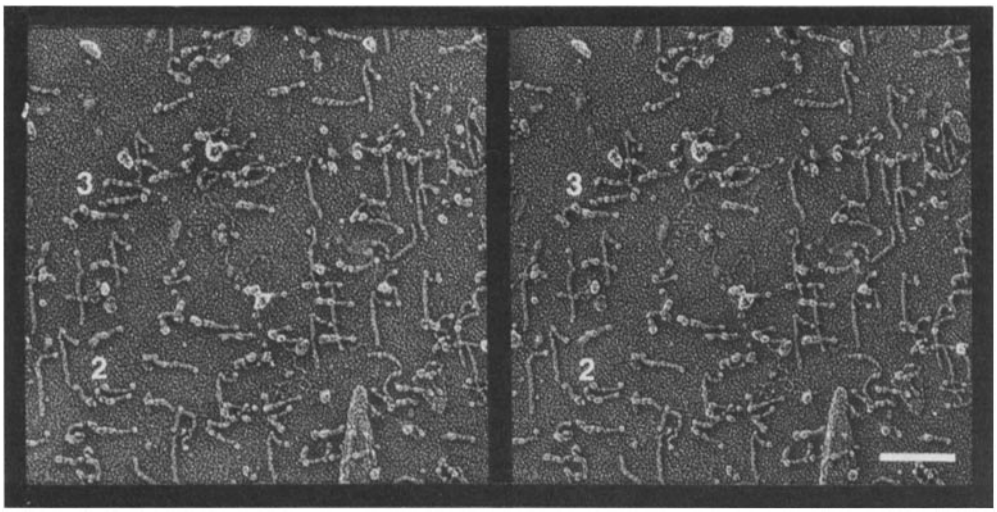

Figure 14. Depolymerized crystal proteins absorbed to mica; stereo pair. Fibrous GP1 molecules orient vertically; GP2 (*2*) and GP3 (*3*) molecules orient horizontally. Bar, 100 nm.

Table II. Amino Acid Composition of Wall Glycoproteins (per 1,000 Residues)

Amino acid	GP1	GP2	GP3	GP1.5
Cys	9.4	15.8	47.0	22.5
Hyp	323.1	147.3	57.4	15.5
Asp	46.6	80.8	105.6	99.2
Thr	42.0	65.9	73.7	43.1
Ser	157.6	82.6	93.3	106.9
Gly	31.5	72.8	74.3	137.9
Pro	27.3	77.4	45.4	31.8
Gly	65.7	85.2	109.6	230.0
Ala	101.4	85.4	102.4	84.0
Val	43.7	56.9	58.5	29.5
Met	8.1	10.4	8.5	4.6
Ile	32.6	12.5	31.9	23.3
Leu	29.2	70.4	69.7	50.5
Tyr	8.9	35.8	11.8	13.7
Phe	12.5	38.2	36.0	22.9
Lys	35.6	30.0	44.6	41.9
His	7.5	2.3	9.6	15.3
Arg	17.4	30.2	20.8	27.4

(reference 13, Figs. 12–14) that *Chlamydomonas* protoplasts first elaborate a radial meshwork of fibers extending from their plasmalemma, after which numerous discrete foci of W6 crystals form within the meshwork at a fixed distance from the cell surface. These foci then enlarge until they become confluent. Possibly, therefore, secreted W6 monomer accumulates within the radial meshwork until it reaches the concentration necessary for crystal formation. A predicted consequence of this mechanism is that the individual growing crystals, unlikely to be in perfect register with one another, will display lattice discontinuities where they meet and join together; we indeed observe such discontinuities in the in situ wall of *C. reinhardtii* (unpublished micrographs), and other species of green algae have been found to display a true platelike organization in their walls (27).

In vitro, monomer concentration will of course be uniform throughout the solution, and wall crystal size is found to be quite uniform as well (Fig. 1). In situ, however, this need not be the case. If, for example, monomer were locally more plentiful, and therefore crystal growth more rapid and extensive, at the cell midline than at the cell poles, then an asymmetric wall could form. The wall of *C. reinhardi*, is, in fact, ellipsoidal rather than spherical, and the related alga *Chlorogonium elongatum* generates a spindle-shaped wall with markedly tapered ends (32). It is attractive to speculate that a similar mechanism might be responsible for generating the very elaborate wall shapes of such algae as the desmids. Meanwhile, this proposal offers a rationale for why the crystalline W6 layer is apparently the first to be assembled during wall formation in *Chlamydomonas* (13)[4]: if this layer indeed establishes the final shape of the wall, then it may serve as a delicate "mold" to dictate the subsequent contours of the underlying layers which, when cross-linked together, appear to provide mechanical stability to the matrix (13, 19, 22).

4. We should note that Fulton (10) concludes, from a thin-section study of the colonial alga *Pandorina morum*, that the outer layer assembles after the inner layer. If experimental differences prove not to explain this discrepancy, then it may be that different constraints govern the assembly of the colony boundary surrounding a group of cells in the Volvocaceae.

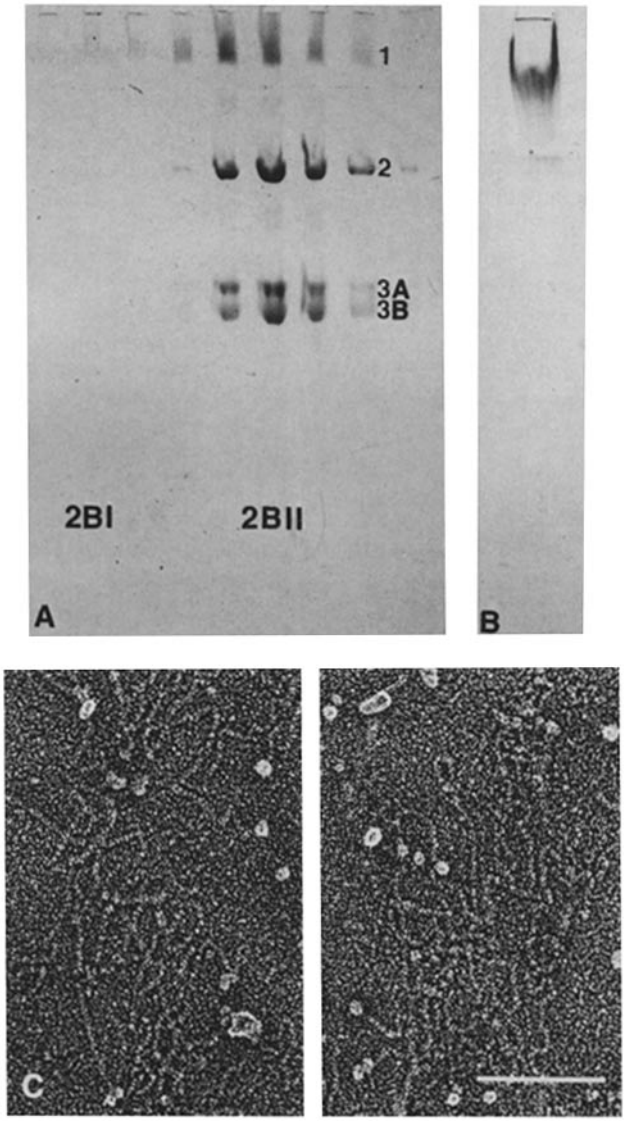

Figure 15. (*A*) SDS PAGE of perchlorate extracts fractionated over a Sepharose 2B column. 2BI and 2BII refer to the two major peaks as defined by Catt et al. (4). Band numbers as in Fig. 6. PAS stain. (*B*) SDS PAGE of the early eluting peaks (before GP3) from a MonoS column (Fig. 8), pooled before electrophoresis. PAS stain. (*C*) Morphology of material in a 2BI fraction, dialyzed against water before adsorption to mica. Bar, 100 nm.

Crystal Stability

We show that the W6-W4-W6 sandwiches are dissociated by the Hofmeister series of chaotropic agents. Such agents may effect solubilization of macromolecules by binding directly to certain groups on the macromolecules (26); alternatively, they may act by changing the structure of the surrounding water (reviewed in reference 35). In their analysis of chaotrope binding to known sites on proteins, Norne et al. (26) conclude that strong halogen binding sites can be characterized as "rigid cavities of relatively hydrophobic character containing positive charges" such as arginine. It is of possible significance in this regard that GP1, GP2, and GP3, the three components of the W6 lattice, bind selectively to cation-exchange columns.

Features of the Purified Cell Wall Glycoproteins

In their original Sepharose 2B fractionation study of *Chlamydomonas* perchlorate extracts, Catt et al. (3) propose that the 2BII fraction contains a single glycoprotein of 298 kD that can be separated into four electrophoretically distinct subunits by SDS PAGE. In subsequent biochemical and structural studies (4, 18, 28, 29), the assumption of a single 2BII glycoprotein continues and in a recent review, Roberts et al. (30) propose the name volvin for this glycoprotein. We show here that the four major electrophoretically separable components of the 2BII fraction (Fig. 15 *A*) are in fact three distinct glycoproteins (Fig. 9), one of which readily dissociates into two subunits upon exposure to β-Me (Fig. 7). Thus it does not seem appropriate to apply a single term to this mixture. Instead, we propose the names GP1, GP2, and GP3 (3A + 3B) for the three major species identified. That these proteins are equivalent to 2BII is reflected in the available data on hydroxyproline composition. Assuming that GP1, GP2, and GP3 each constitute ⅓ of the 2BII fraction (c.f. Fig. 6), then the values in Table II dictate that a mixture of the three would contain 17.6% hydroxyproline, which is similar to Catt et al.'s (4) estimate of 15% hydroxyproline for the 2BII material.

By morphology, the GP2 and GP3 glycoproteins are clearly related, with a fibrous domain associated with two or more globular domains (Figs. 12 and 13). The globular domains presumably form the globular units of the W6A crystalline lattice (Fig. 5) and the fibrous domains form the interconnecting straight domains (cf. reference 13, Fig. 17, and reference 28); exactly how these proteins interact to generate the lattice is the subject of a separate study.[2] The fibrous domains of GP2 and GP3 are also structurally similar to the knobbed end of the GP1 glycoprotein: all are 25–28-nm long and bear a similar knob at one end. Thus it is attractive to speculate that the three species evolved as a consequence of gene fusions between a common hydroxyproline-rich sequence and dissimilar sequences dictating either globular domains (GP2 and GP3) or a second fibrous domain (GP1). We have initiated cloning experiments to identify the genes for these proteins; their sequences will clearly address this and other questions about the evolution of this protein family (see also references 7 and 11 for a discussion of similarities between wall proteins and the sexual agglutinin of *Chlamydomonas*).

It is of some interest that the GP3 species is composed of two glycopolypeptides conjoined by linkages that are sensitive to β-Me and to 100°C, whereas its apparent homologue GP2 appears to be a single glycopolypeptide chain. A similar situation has recently been described for two hormone receptors: the EGF receptor functions as a single 170-kD polypeptide (6), whereas the insulin receptor, synthesized as a 180-kD polypeptide with domains homologous to the EGF receptor (8), is subsequently cleaved into two subunits that are then linked together by β-Me-sensitive bridges (33).

In whole-wall extracts that form W6-W4-W6 sandwiches, a fourth glycopolypeptide is present, in lesser amounts, which migrates between GP1 and GP2 by SDS PAGE. We propose the name GP1.5 for this species, and suggest that it forms the granules that lie between the W6 layers in these sandwiches (Fig. 4) and that lie between the W6 and W2 layers in situ (13). Its central position initially suggested to us that it might cause the formation of sandwiches by cross-bridging two W6 layers together. However, we have recently found that the proteins retained on our cation-exchange columns form crystal sandwiches in the absence of any GP1.5, with the two W6 layers simply conjoined by fibrous strands. Therefore, GP1.5 proteins apparently recognize binding sites within the sandwiches but are not required for sandwich assembly. Consistent with this conclusion, we note considerable variability in the amount of granular material within individual crystal sandwiches, and a highly variable amount of GP1.5 in various crystal preparations.

The globular structure of GP1.5 and its low hydroxyproline content place it in a distinct genetic category from the other wall glycoproteins. It contains 23% acidic amino acids and sticks avidly to anion-exchange columns, whereas the W6 glycoproteins have no affinity for anion-exchange resins. Therefore, GP1.5 may associate with the W6 glycoproteins, at least in part, on the basis of charge.

Finally, we should note that minor glycopolypeptide bands 2.1 and 2.2, plus a minor band running near the front of our SDS PAGE system, are also consistent components of the in vitro crystals (13; and Figs. 6 and 7 of this study). One possibility is that they represent proteolytic fragments of higher molecular weight species. If they instead prove to be bona fide wall components, then their stoichiometries suggest that they will prove to play a role in initiating and/or stabilizing crystal formation rather than serving as structural elements of the lattice.

With the major glycoproteins now purified, we can in future experiments ask what any kinds of molecular aggregates will form in vitro if various subsets of the matrix are co-incubated. We can also ask whether *Chlamydomonas* monomers can co-crystalize with monomers derived from other matrixes, e.g., the W6 layer of *Volvox* (20).

We warmly thank Valerie Mermall for the SDS PAGE, Carol Hwang for cell cultures, Robyn Roth for replicas, Comfree Coleman and Dianne Mattson for photography, and Ann Dillon for artwork.

This work was supported by grants GM-26150 to U. W. Goodenough, HL-26499 to R. P. Mecham, and GM-29657 to J. E. Heuser.

Received for publication 10 March 1986, and in revised form 5 May 1986.

References

1. Adair, W. S., B. C. Monk, R. Cohen, and U. W. Goodenough. 1982. Sexual agglutinins from the *Chlamydomonas* flagellar membrane: partial purification and characterization. *J. Biol. Chem.* 256:4593–4602.

2. Bornstein, P., and H. Sage. 1980. Structurally distinct collagen types. *Annu. Rev. Biochem.* 49:967–1003.

3. Catt, J. W., G. J. Hills, and K. Roberts. 1976. A structural glycoprotein, containing hydroxyproline, isolated from the cell wall of *Chlamydomonas reinhardi*. *Planta.* 131:165–171.

4. Catt, J. W., G. J. Hills, and K. Roberts. 1978. Cell wall glycoproteins from *Chlamydomonas reinhardi*, and their self-assembly. *Planta.* 138:91–98.

5. Chen, L. B., editor. 1981. Oncology Overview: Selected Abstracts on Fibronectin and Related Transformation-Sensitive Cell Surface Proteins. Intl. Cancer Res. Data Bank, Natl. Cancer Inst., Bethesda, MD.

6. Cohen, S., G. Carpenter, and L. E. King, Jr. 1980. Epidermal growth factor-receptor-protein kinase interactions. Co-purification of receptor and epidermal growth factor-enhanced phosphorylation activity. *J. Biol. Chem.* 255:4834–4842.

7. Cooper, J. B., W. S. Adair, R. P. Mecham, J. E. Heuser, and U. W. Goodenough. 1983. *Chlamydomonas* agglutinin is a hydroxyproline-rich glycoprotein. *Proc. Natl. Acad. Sci. USA.* 80:5898–5901.

8. Ebina, Y., L. Ellis, K. Jarnagin, M. Edery, L. Graf, E. Clauser, J. Ou, F. Masiarz, Y. W. Kan, and W. J. Rutter. 1985. The human insulin receptor cDNA: the structural basis for hormone-activated transmembrane signalling. *Cell.* 40:747–758.

9. Ekblom, P., E. Lehtonen, L. Saxen, and R. Timpl. 1981. Shift in collagen type as an early response to induction of the metanephric mesenchyme. *J. Cell Biol.* 898:276–283.

10. Fulton, A. B. 1978. Colonial development in *Pandorina morum* II. Colony morphogenesis and formation of the extracellular matrix. *Dev. Biol.*

64:236–251.

11. Goodenough, U. W., W. S. Adair, P. Collin-Osdoby, and J. E. Heuser. 1985. Structure of the *Chlamydomonas* agglutinin and related flagellar surface proteins in vitro and in situ. *J. Cell Biol.* 101:924–941.

12. Goodenough, U. W., and J. E. Heuser. 1984. Structural comparison of purified dynein proteins with in situ dynein arms. *J. Mol. Biol.* 180:1083–1118.

13. Goodenough, U. W., and J. E. Heuser. 1985. The *Chlamydomonas* cell wall and its constituent glycoproteins analyzed by the quick-freeze deep-etch technique. *J. Cell Biol.* 101:1550–1568.

14. Hay, E. D. 1983. Cell and extracellular matrix. Their organization and mutual dependence. *Mod. Cell Biol.* 2:509–548.

15. Heuser, J. E. 1980. Three-dimensional visualization of coated vesicle formation in fibroblasts. *J. Cell Biol.* 84:560–583.

16. Heuser, J. E. 1983. Procedure for freeze-drying molecules adsorbed to mica flakes. *J. Mol. Biol.* 169:155–195.

17. Hills, G. J., J. M. Phillips, M. R. Gay, and K. Roberts. 1975. Self-assembly of a plant cell wall in vitro. *J. Mol. Biol.* 96:431–441.

18. Homer, R. B., and K. Roberts. 1979. Glycoprotein conformation in plant cell walls. *Planta.* 146:217–222.

19. Imam, S. H., M. J. Buchanan, H.-C. Shin, and W. J. Snell. 1985. The *Chlamydomonas* cell wall: characterization of the wall framework. *J. Cell Biol.* 101:1599–1607.

20. Kirk, D. L., R. Birchem, and N. King. 1986. The extracellular matrix of *Volvox*: a comparative study and proposed system of nomenclature. *J. Cell Sci.* 80:207–231.

21. Lamport, D. T. A. 1980. Structure and function of glycoproteins. *In* The Biochemistry of Plants. Vol. 3. J. Preiss, editor. Academic Press, Inc., New York. 501–541.

22. Matsuda, Y., T. Saito, T. Yamaguchi, and H. Kawase. 1985. Cell wall lytic enzyme released by mating gametes of *Chlamydomonas reinhardtii* is a metalloprotease and digests the sodium perchlorate-insoluble component of cell wall. *J. Biol. Chem.* 260:6373–6377.

23. Mecham, R. P., and G. Lange. 1982. Antigenicity of elastin: characterization of major antigenic determinants on purified insoluble elastin. *Biochemistry.* 21:669–673.

24. Monk, B. C., W. S. Adair, R. A. Cohen, and U. W. Goodenough. 1983. Topography of *Chlamydomonas*: fine structure and polypeptide components of the gametic flagellar membrane surface and the cell wall. *Planta.* 158:517–533.

25. Morrissey, J. H. 1981. Silver stain for proteins in polyacrylamide gels: a modified procedure with enhanced uniform sensitivity. *Anal. Biochem.* 117:307–310.

26. Norne, J.-E., S.-G. Hjalmarsson, B. Lindman, and M. Zeppezauer. 1975. Anion binding properties of human serum albumin from halide ion quadrupole relaxation. *Biochemistry.* 14:3401–3408.

27. Roberts, K. 1974. Crystalline glycoprotein cell walls of algae: their structure, composition, and assembly. *Philos. Trans. R. Soc. Lond. B Biol. Sci.* 268:129–146.

28. Roberts, K. 1981. Visualizing an insoluble glycoprotein. *Micron.* 12: 185–186.

29. Roberts, K. 1979. Hydroxyproline: its asymmetric distribution in a cell wall glycoprotein. *Planta.* 146:275–279.

30. Roberts, K., C. Grief, G. J. Hills, and P. J. Shaw. 1985. Cell wall glycoproteins: structure and function. *J. Cell Sci. Suppl.* 2:105–127.

31. Roberts, K., M. Gurney-Smith, and G. J. Hills. 1972. Structure, composition, and morphogenesis of the cell wall of *Chlamydomonas reinhardi*. I. Ultrastructure and preliminary chemical analysis. *J. Ultrastruct. Res.* 40: 599–613.

32. Roberts, K., and G. J. Hills. 1976. The crystalline glycoprotein cell wall of the green alga *Chlorogonium elongatum*: a structural analysis. *J. Cell Sci.* 21:59–71.

33. Ronnett, G. V., V. P. Knutson, R. A. Kohanstzi, T. L. Simpson, and M. D. Lane. 1984. Role of glycosylation in the processing of newly translated insulin proreceptor in 3T3-L1 adipocytes. *J. Biol. Chem.* 259:4566–4575.

34. Trelstad, R. L., editor. 1984. Role of Extracellular Matrix in Development. Alan R. Liss, Inc., New York. 643 pp.

35. van Hippel, P. H., and T. Schleich. 1969. Ion effects on the solution structure of biological macromolecules. *Accts. Chem. Res.* 2:257–265.